

The Effect of Transverse Shifts on the LIGO Interferometer (Simulation Study)

Document Number: LIGO-T050181-00-E

Author: Doug Fetting
Mentor: Biplab Bhawal

Abstract:

The LIGO interferometers have reached their designed sensitivity level which is greater than any other interferometer ever built. At this point, it is important to have a proper understanding of small perturbations that might still exist (until now these issues did not come to the forefront because other more critical problems needed to be solved in order to approach the expected designed level of sensitivity). This project focuses on how possible existence of transverse shifts in either beam or optics would affect the alignment and sensitivity of these detectors. Two simulation tools are used for this purpose: The time domain simulation package called End-to-End (E2E) model and a static FFT code developed for LIGO. The results are analyzed to look for changes in noise curves, recycling gain, beam intensity profiles etc for both the laser carrier frequency and sideband frequencies. The asymmetries in beam profiles are also looked at to evaluate the effect of such perturbations on alignment sensing.

Introduction

The Laser Interferometer Gravitational-Wave Observatory (LIGO) is an on going project to measure the gravitational radiation predicted by general relativity. According to Albert Einstein's theory of general relativity, gravity can be thought of as a curvature of space-time. Einstein's theory predicts that when massive stellar objects are accelerated in a sufficient manner, ripples of space time will be emitted from the motion, i.e. gravity waves. These waves should propagate across the universe at the speed of light, but with exceedingly small amplitude. In fact, the amplitude is so small that some scientist thought that gravitational waves may never be detected, and so far they're correct. However, LIGO's sensitivity is becoming very close to the sensitivity needed to detect some of the gravitational waves thought to be detectable on Earth^[1].

Potential sources for such gravitational waves include: compact binary systems with either neutron stars, black holes, or both; rotating neutron stars; supernovae; super massive black holes; the stochastic background from the early universe and big bang. Detection of gravitational waves from any of these sources would allow scientists to have a completely new look at these phenomena as well as the first look at a gravitational wave. As of now scientists have only viewed the universe through electromagnetic radiation, or light, and gravitational waves are a different form of radiation which can contain information that is unobtainable from light. In particular, gravitational waves from the big bang would give a first look at the early universe, one that is not possible with electromagnetic radiation^[2].

Detection of Gravitational Waves

The detection of gravitational waves is a very complex and difficult process with many physical hurdles. For example, it is necessary to have multiple detectors at sites separated by a large distance. As a result, there are LIGO facilities in both Hanford, Washington and Livingston, Louisiana. Each of the detectors is essentially a large Michelson interferometer, which has two identical arms of 4 km in an L-shape (see Figures 1 & 2). The idea behind the detector is that it can measure the length of each of the arms very precisely. If a gravitational wave passes through the detector, the arms will change length accordingly and this change can effectively detect the wave. The sensitivity of LIGO will be around 10^{-18} , which is about 1/1000 the size of an atomic nucleus. This sensitivity would be sufficient to detect such events as a Supernovae in our galaxy or a binary collision of two 1.4 solar mass objects like neutron stars or black holes^[3].



Figure 1 *Overhead view of Hanford detector. Notice the L-shape and the immense 4km arms.*

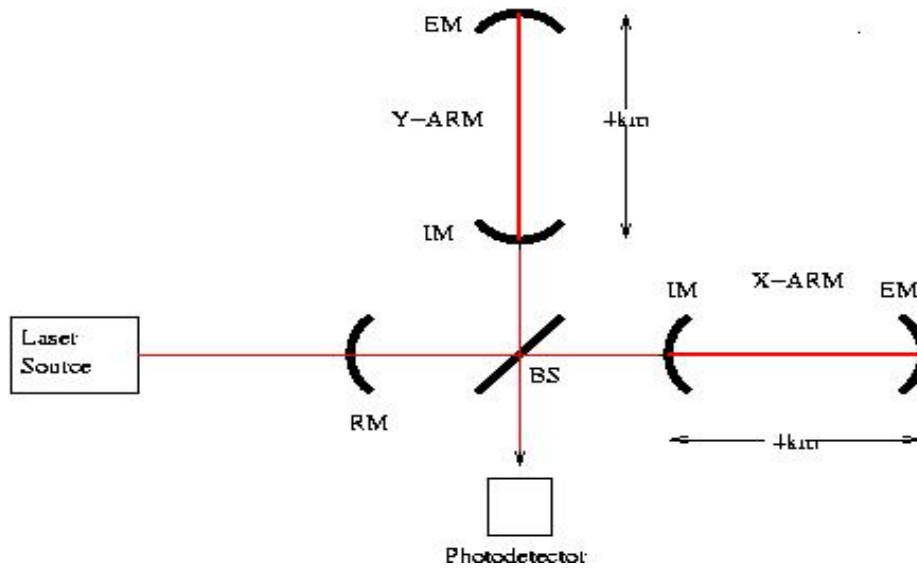
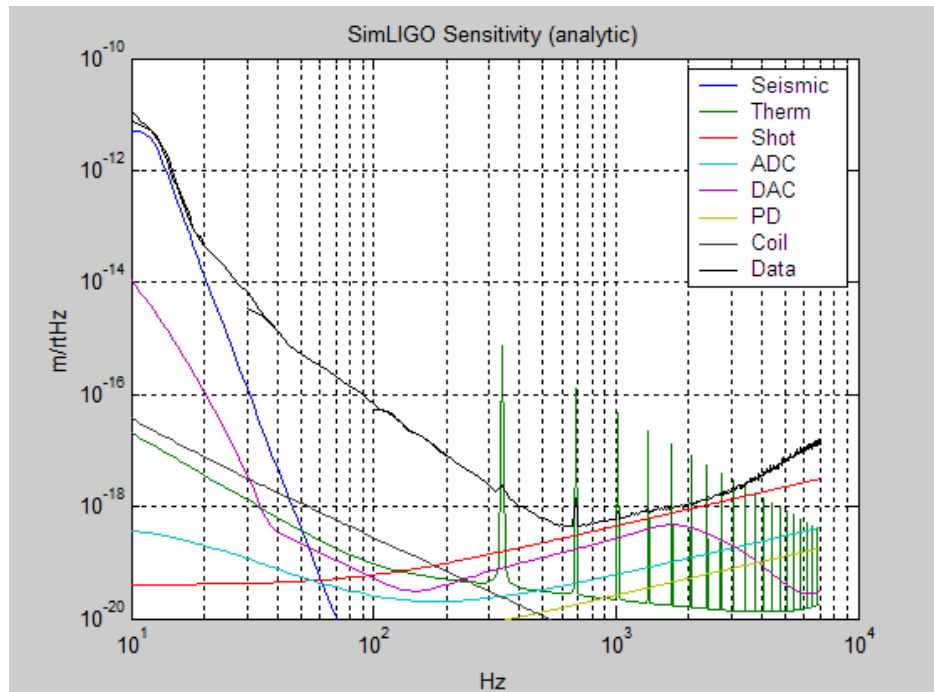


Figure 2 Each arm has a two mirror cavity, called a Fabry-Perot cavity. There is a laser beam that passes through each of the arms and resonates in the cavities. The laser light is phase modulated and actual consists of three prominent frequencies; a central frequency, called the carrier frequency, and two frequencies which are equally above and below the carrier beam, known as the upper and lower sidebands.



Graph 1 LIGO Hanford sensitivity curve generated by SimLIGO. The black curve shows the sensitivity of the interferometer at different frequencies. The other colored curves represent the different noise sources found in LIGO. The three main sources are seismic noise, thermal noise, and shot/quantum noise. This curve was made using a higher noise assumption compared to the curve in graph 4.

To measure a distance this small, it is necessary to reduce the noise in the system to a value less than this. LIGO is set to detect waves in the frequency range of 100 Hz to 1000 Hz with the highest sensitivity at about 200 Hz. Therefore all types of noise at these frequencies must be dealt with. Graph 1 above shows a noise and sensitivity curve generated by SimLIGO for the LIGO detector in Hanford. The graph shows many different sources of noise in the detector between 10 Hz and 10000 Hz. The black curve is the actual sensitivity of the detector which is limited by seismic noise at low frequencies and shot noise at high frequencies. As one can see from the graph, the detector is most sensitive around 10^2 Hz to 10^3 Hz. It is designed to be so because the binary coalescence signals have their highest signal-to-noise ratio in that frequency range^[3].

Transverse Shifts

The LIGO interferometers are the most sensitive interferometers in the world. To reach such a high sensitivity, much effort has been put into reducing the noise in the interferometers. Seismic noise, thermal noise, and shot noise determine the detector's sensitivity in different frequency regions. Until recently small perturbations in transverse directions have been unimportant in comparison with other noise issues. However, as the sensitivity of the interferometer increases these transverse perturbations may become more important. Also, there is some evidence that suggests that one of the mirrors in the Hanford detector is shifted by 1-2cm from the expected position and that the laser beam can be shifted by up to 1cm at times.

Figures 3a and 3b show an example of a transverse shift. The situation shown in figure 3a will be referred to as the unperturbed or base case. Figure 3b shows the

situation where all five of the mirrors are shifted by 1 cm. When in detection mode, the interferometer is said to be in a ‘locked’ state. This refers to the fact that the interferometer has a preferential state where the light in the cavities will be resonant and the power in the arms will be very high, about 15 kW.

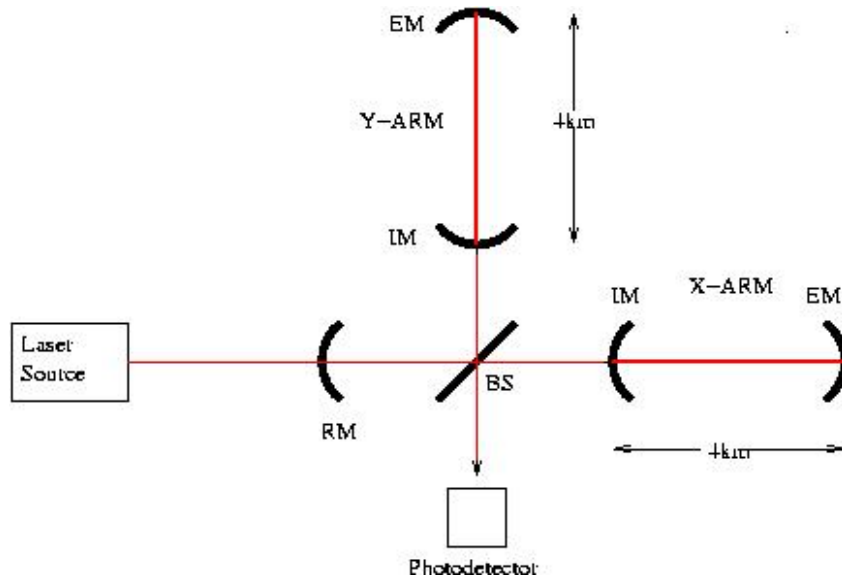


Figure 3a *Diagram showing the mirrors of the LIGO detector in the unperturbed or normal state.*

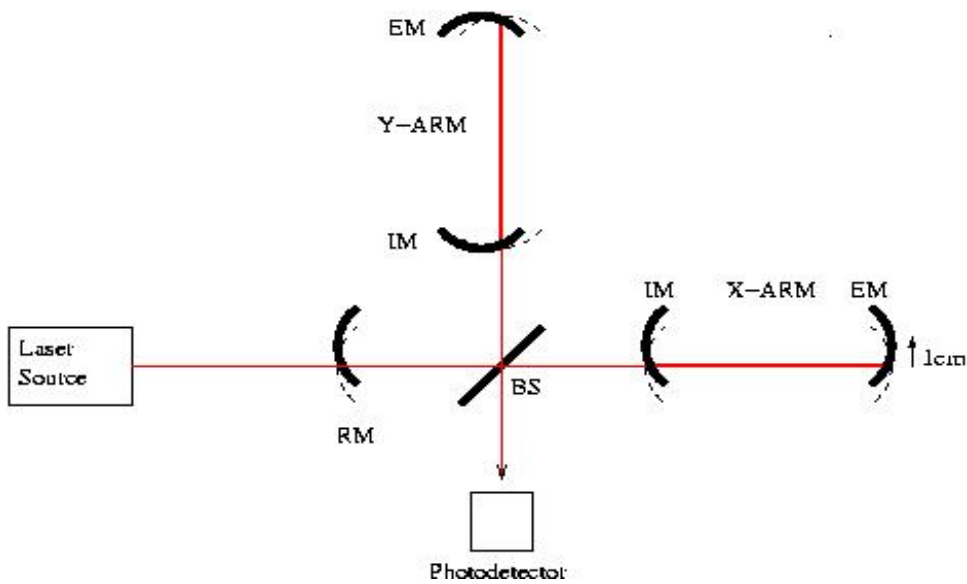


Figure 3b *Diagram showing the LIGO detector with a transverse shift of 1cm to all of the optics.*

The purpose of my summer project is to determine the effects of transverse shifts on LIGO's interferometers. Through computer simulation the aim of this project is to create a map of how various shifts to the mirrors and the laser beam affect the interferometer's performance. Two different, independent simulation programs are utilized in the project; End-to-End or E2E and the FFT code developed by MIT. To study the effects of transverse shifts it is first useful to know about the wavefront sensors in the LIGO detectors and about how angular rotations of the mirrors are equivalent to transverse shifts.

Figure 4 illustrates the basic geometry on how a rotation of the mirror can have the same effect as shifting the mirror. Using this idea it is actually possible to counteract a shift in a mirror by rotating that mirror by a specific amount. The angle of rotation about the x-axis is called pitch and rotation about the y-axis is known as yaw. The exact relations can be easily derived and are

$$\text{(Equations 1 \& 2)} \quad Yaw = \frac{dx}{R} \quad Pitch = -\frac{dy}{R}$$

where R is the radius of curvature of that given mirror and dx (dy) is the shift in the horizontal (vertical) direction. For example, if a mirror is shifted by 1cm in the horizontal direction, with a radius of curvature of about 14,000m, this corresponds to

$$Yaw = \frac{0.01m}{14000m} \approx 7 * 10^{-7} \text{ rad}$$

Therefore, in order to counteract this shift a rotation of $-7 * 10^{-7}$ rad is needed (notice the minus sign.) The divergence angle for the laser beam, which represents a large angle for this situation, is about $1 * 10^{-5}$ rad, which is about 15 times greater than the rotation of the mirror.

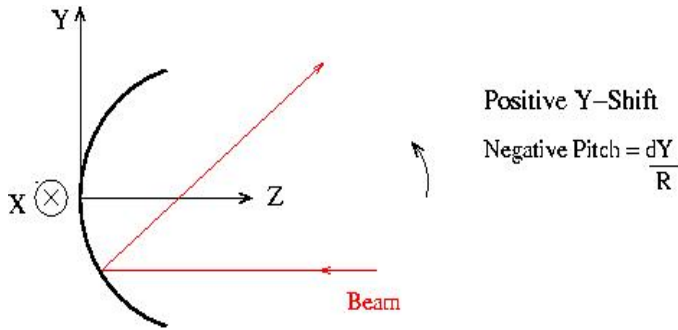


Figure 4 Geometrical diagram showing why rotating the mirrors can have the same effect as shifting the mirrors. The light reflects at the same angle that it was incident on the mirror, thus one can rotate the shifted mirror so that it will be perpendicular to the beam, reflecting it straight back.

. The wavefront sensors can detect a shift in the laser beam by sensing asymmetries in the intensity distribution, as illustrated in figure 5. There are several wavefront sensors located throughout the detector so that a shift anywhere in the detector can be located. When the wavefront sensors detect a shift in the beam, the control system will then try to correct the shift by rotating the mirror(s) as explained previously. Note that the actual wavefront sensors are able to detect shifts in both transverse directions whereas the sensor in figure 5 only shows detection for one direction.

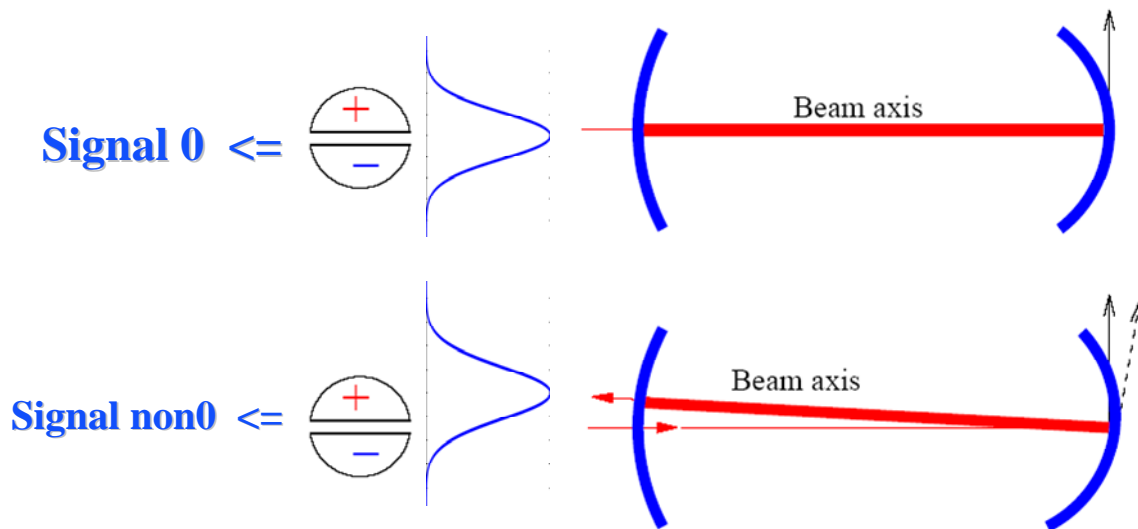


Figure 5 Wavefront sensors detect shifts in the beam by subtracting the intensities on either side of the central axis. If the beam is centered correctly the detectors will have a reading of 0, but if the beam is off-center a non-zero reading will be given. Diagram provided by Biplab Bhawal.

Simulation Experiments and Results

For these experiments two separate simulation packages were used. The first simulation tool is the FFT code developed by MIT which is a static, frequency domain environment. That is, it runs the simulations and gives its results in a steady state. Each mirror in the FFT code is represented by a 128x128 grid where each box contains the imaginary and real parts of the electromagnetic field located at the mirror, i.e. the laser beam. Using this grid it is easy to view the laser beam's distribution on the mirror. For example, the plots shown in graph 2 are a cross-section of such a grid^[4].

The second simulation code is the end-to-end or E2E simulation package. E2E is a time domain modal model that was developed specifically for simulating a variety of situations that could be useful for improving LIGO. SimLIGO was developed in the E2E environment and is a very complex model of the actual LIGO interferometers. SimLIGO includes most of the optics, suspension and mechanical systems, control and feedback systems and noise sources that are found in the actual detectors^[5].

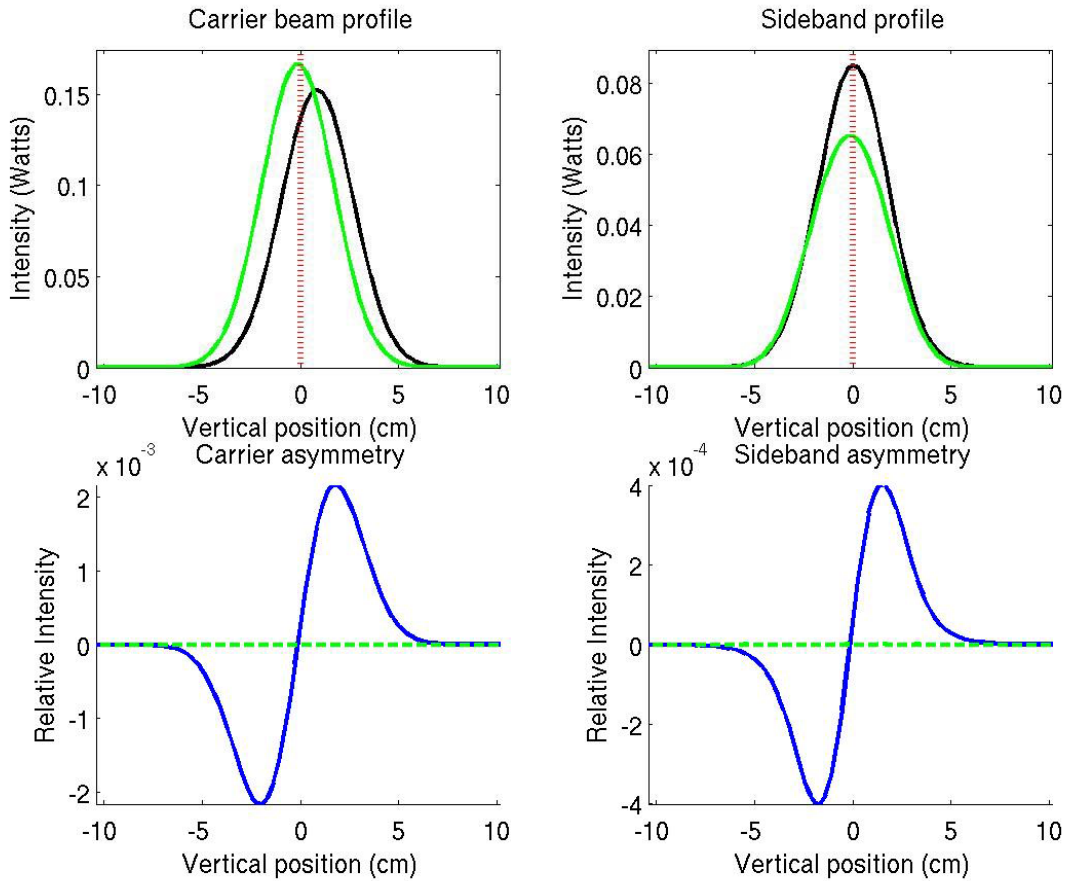
Because of its time domain nature and complexity, the SimLIGO simulations took much more computation time than those done with the FFT code by about a factor of 50. Also, the results from the FFT code are usually more accurate than those from E2E. On the other hand, because of both its time domain nature and complexity the E2E simulations provide a plethora of information about the interferometer that is unobtainable from the FFT simulations. Thus, for a complete view on these simulations, it is beneficial to use both simulation tools.

When shifting all of the mirrors vertically by 1cm, the relative position of all of the mirrors to all of the other mirrors is exactly the same as the unperturbed case.

However, with respect to the laser beam and the wavefront sensors everything has been shifted up by 1cm. Therefore the center of the mirrors and the resonant cavity that they define are no longer located along the central axis. Graph 2 shows data obtained at the input to the recycling cavity from a simulation done with the FFT code.

In the upper left plot of graph 2, the carrier beam is shifted in the perturbed case by about 1cm with respect to both the central axis and the unperturbed case. This is expected because the mirrors in the detector are in such a way that they define a resonant cavity for the carrier and therefore the carrier will follow the cavity. The sideband, as seen in the upper right graph, doesn't shift as the carrier did because even though it is resonant in the cavity it's also very close to the unstable condition in the cavity. Under such a condition the sideband will not shift with the cavity. The bottom two graphs show the relative asymmetries around the central axis which is similar to what the wavefront sensor would detect.

A way to check the reasoning and predictions obtained from the above data would be to run a simulation where the laser beam is instead shifted *down* 1cm and the mirrors are left unperturbed. Such a run was simulated and the results were consistent with those obtained above, that is the carrier was not shifted because it follows the cavity and the sideband was shifted by -1cm because it followed the laser. These simulations were done without the feedback and control system activated. In a real situation, these shifts would be corrected by rotating the mirrors as discussed previously. To simulate such a feedback correction, I used the E2E simulation package.



Graph 2 *The top row shows the intensity profile of the laser beam after the entrance to the recycling cavity. The carrier profile is shown on the left and the upper sideband profile is shown on the right, where the green line is from the unperturbed case, the black line is from the shifted case and the red line represents the central axis where the wavefront sensor would be centered. The bottom row shows the asymmetries of the top curves.*

The diagram in figure 6 shows how one would expect the interferometer to respond to a transverse shift in the mirrors. The exact amount that each mirror should be rotated can be calculated from the formulas for pitch and yaw shown previously. To test these predictions a simulation was ran in E2E where the interferometer was first allowed to achieve the locked state and then the mirrors were shifted. The shift to the mirrors had to be done over an extended period of time or else the interferometer would go out of lock. Notice how these precautions were not necessary for the FFT simulation.

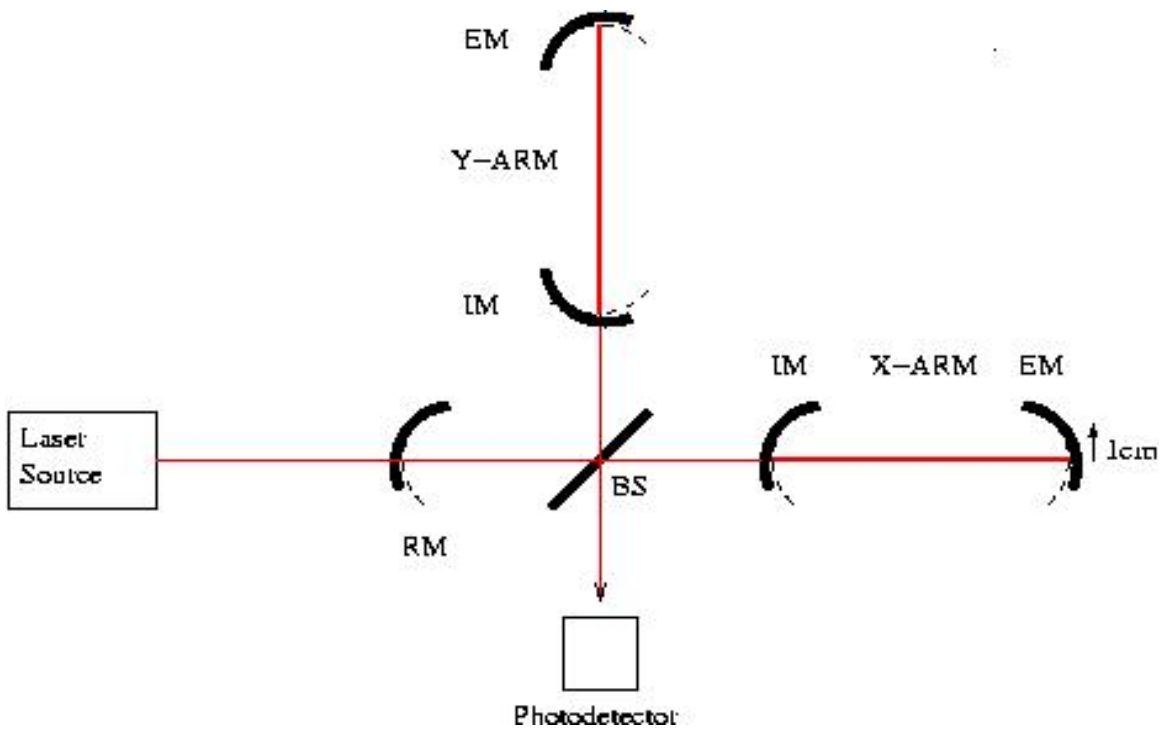
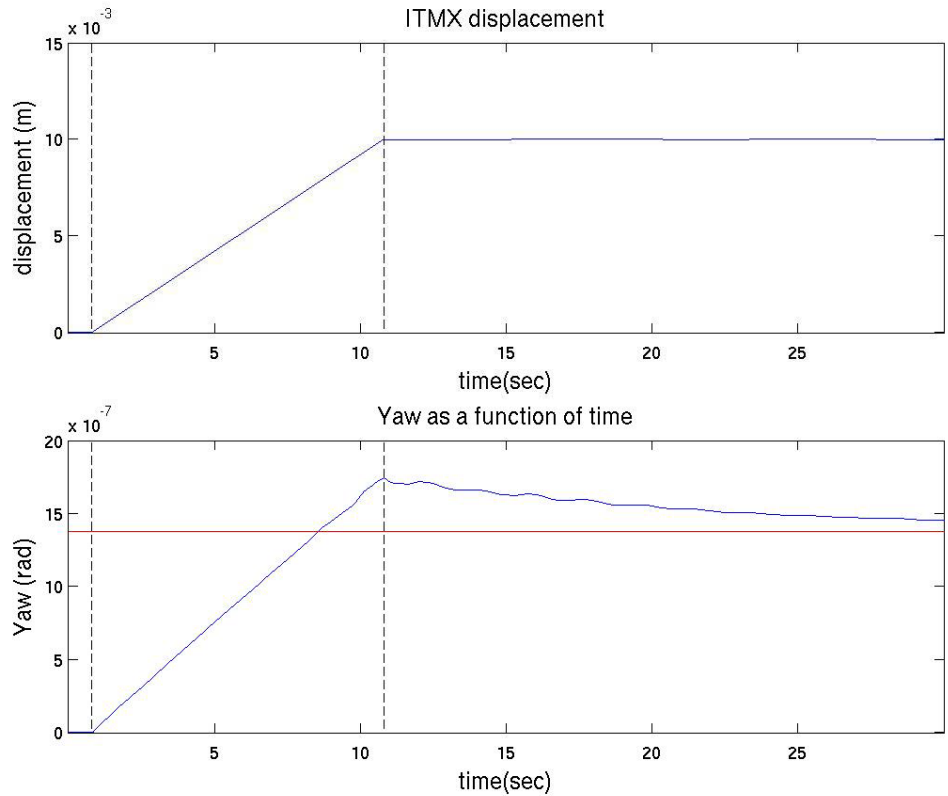


Figure 6 *Diagram of how the detector should rotate the mirrors in response to a 1cm shift. Notice how the curved mirrors are perpendicular to the beam after the rotation.*

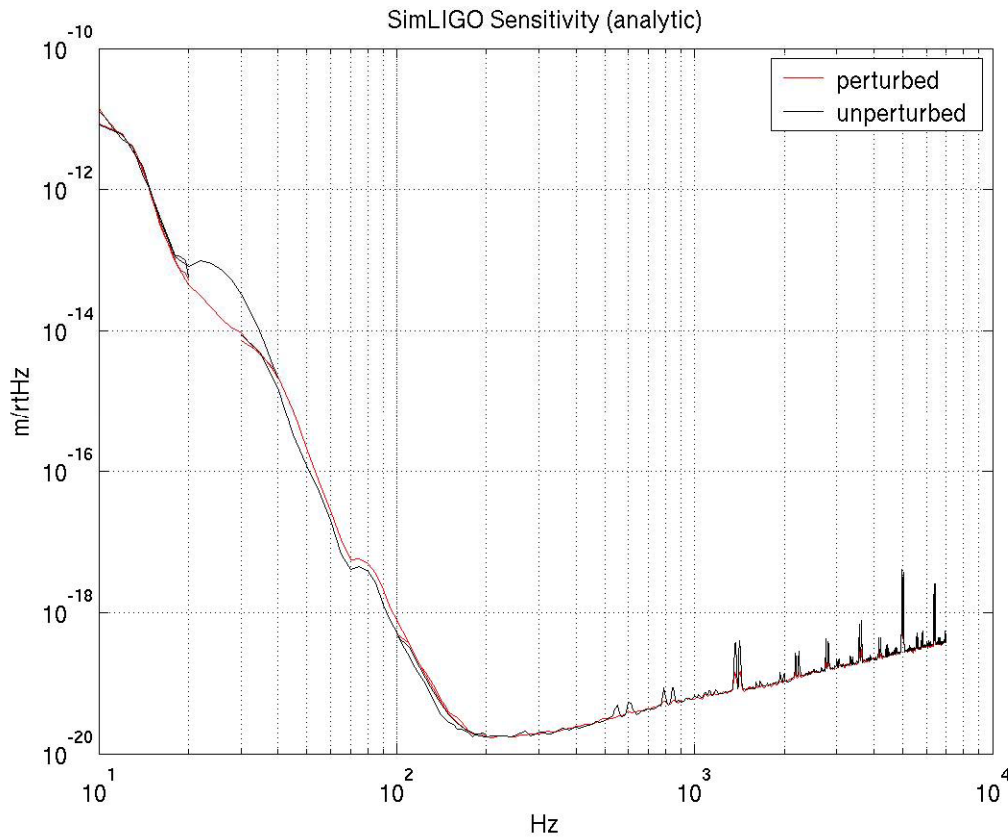
The upper plot of graph 3 shows how the shift to the mirror was performed. The interferometer was given about 0.7 sec to build the power up to the saturation level. Then the mirror was continuously shifted over a 10 sec period for a total distance of 1cm. The lower plot shows how one of the mirrors was rotated over this time period and the predicted value of rotation. In the lower plot of graph 3 the actual rotation is shown to first go above the predicted value and then settles back down. This is most likely caused by the control system first overcompensating for the shifts and then adjusting back once the shifting has ceased.



Graph 3 *The upper plot shows how the ITMX mirror move in the x-direction as a function of time. The two dotted line represent when the movement started and stopped. The bottom plot shows the yaw of the same mirror over the same time period with the blue curve. The red line is the theoretical value that the mirror should eventually attain. Notice how the interferometer had about 0.7sec to build up power before the mirror started moving.*

It has been predicted that a small angular perturbation of the mirrors on the order of $0.01 \mu\text{rad}$ should cause the shot noise sensitivity to decrease by about 0.5%^[6].

Graph 4 shows the sensitivity curve for this simulation. One can see that at higher frequencies, where the increased shot noise would show its effects, there seems to be no difference between the perturbed and unperturbed situations. These results suggest that the control system does correctly adjust the pitch/yaw for each mirror to cancel out any transverse shifts. Also, the actual rotations are very close to the predicted values and the rotations do not appear to increase the shot noise.



Graph 4 *Shows the sensitivity of the interferometer as a function of frequency. The black line represents the unperturbed case and the red line represents the perturbed case. At lower frequencies the red curve is actually below the black curve, which is probably due to some numerical inaccuracies. At higher frequencies the two curves are very similar, indicating no increase in the shot noise for the perturbed case. Note that this graph was made using a lower noise assumption than the curve shown in graph 1.*

Methods

FFT Simulation Package

The FFT code developed by MIT is a simulation tool that has been in use for several years and is used for many different reasons. In the process of using the FFT package, a bug in the code was found that was preventing the mirrors from shifted correctly. This bug wasn't noticed until now because no one has studied these shifts with FFT. The bug has now been fixed and the FFT code correctly shifts the mirrors as one would expect it to. Also, the coordinate system used for the shifting of the mirrors in the FFT package is not well documented. Therefore, a simple sketch of the coordinate axes at each mirror has been included in figure 7.

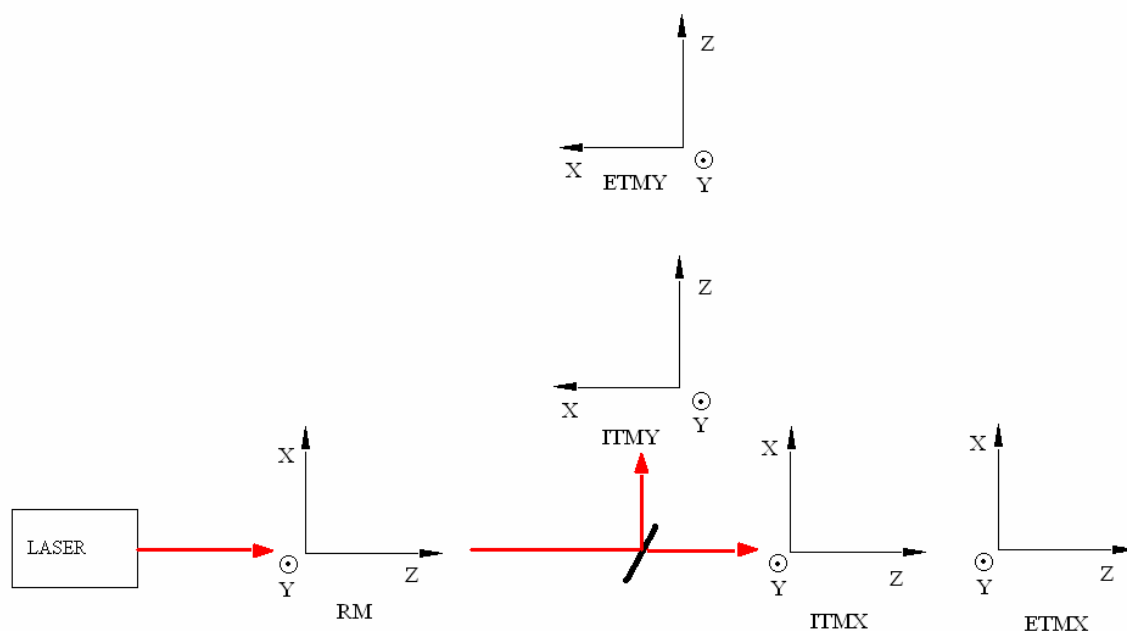


Figure 7 *A simple sketch of the coordinate system used at each mirror in the FFT code. The z-axis is always along the direction of propagation for the input laser beam (the red line). The y-axis is always pointing up and the x-axis is determined from the right-handed nature of the coordinate system. The coordinate system is in reference to the laser beam, so it is independent of which side of the mirror one is looking from.*

Additional simulations

In addition to the FFT simulations already discussed, several other simulations were done that are worth mentioning. Table 1 shows results from several of the runs. By looking at the recycling gain of each situation, one can compare the different runs and see that the unperturbed case, run #1, and runs #2, 3, 8, 9, 12, 13 all have gains within about 2% of each other. These are all cases where something was shifted and then that shift was corrected, either by rotating the mirrors or shifting the laser. This result is consistent with the results discussed previously. Also, the results of the simulations are direction independent because any shift in the x-direction has a corresponding shift in the y-direction with an almost identical recycling gain. These two conclusions agree well with prior predictions and therefore make the original results more credible.

Run #	Shifted	Rotated	Direction	Recycling Gain
1	None	None	None	46.06
2	All mirrors and Laser	None	Horizontal (x)	46.28
3	All mirrors and Laser	None	Vertical (y)	46.09
4	Laser	None	Horizontal (x)	42.24
5	Laser	None	Vertical (y)	42.25
6	All mirrors	None	Horizontal (x)	42.38
7	All mirrors	None	Vertical (y)	42.21
8	All mirrors	All mirrors	Horizontal (x)	45.00
9	All mirrors	All mirrors	Vertical (y)	45.00
10	ITMX only	None	Horizontal (x)	41.54
11	ITMX only	None	Vertical (y)	41.48
12	ITMX only	ITMX	Horizontal (x)	46.13
13	ITMX only	ITMX	Vertical (y)	46.13

Table 1 *The above table shows results from several different simulations done with FFT. The ‘shifted’ column tells which components were shifted, the ‘rotated’ column shows which components were rotated and the direction column shows which direction the shifting was done in. The recycling gain column indicates what the gain was in the recycling cavity for a given simulation.*

Acknowledgements

I would like to thank Biplab Bhawal for being a great mentor and helping me out with any questions I had on the project and this paper. I would like to thank the NSF for funding me on this project, and the LIGO/SURF program and Kenneth Libbrecht for making this opportunity possible.

References

- [1] Sigg, Daniel. *Gravitational Waves*. Proceedings of Tasi 98. 1 – 5 (1998).
- [2] Sigg, Daniel. *Gravitational Waves*. Proceedings of Tasi 98. 6 – 11 (1998).
- [3] Bhawal, Biplab. *Physics of interferometric gravitational wave detectors*. Pramana, 646-648 (2004).
- [4] Bhawal, Evans, Rakhmanov, and Yamamoto. *Time Domain Modal Model in End-to-End simulation package*. 4 (2004).
- [5] Bochner, Brett. *Modelling the Performance of Interferometric Gravitational-Wave Detectors with Realistically Imperfect Optics*. MIT PhD Thesis, June 1998.
- [6] Fritschel, Peter. *Alignment Sensing/Control Design Requirements Document*. LIGO, p. 10 (1997).